Ligand-Based Redox Reactions. Analysis of the Electron Paramagnetic Resonance Spectrum of the $[Ni(Me_4[14]hexaenatoN_4)]^+$ Cation Radical, the Central Member of a Three-Membered Electron Transfer Series Containing a Tetraaza[14]annulene Ligand System

Michelle Millar and R. H. Holm*

Contribution from the Department of Chemistry, Massachusetts Institute of Technology, Cambridge, Massachusetts 02139. *Received March 14, 1975.*

Abstract: Previous investigation of the tetraaza macrocyclic metal(II) complexes $M(Me_4[14]tetraenatoN_4)$ has shown that they can be oxidatively dehydrogenated to $[M(Me_4[14]hexaenatoN_4)]^+$. Monocations containing M = Ni, Pd, and Cu can be oxidized and reduced affording the three-membered electron transfer series $[M(L)]^0 \rightleftharpoons [M(L)]^+ \rightleftharpoons [M(L)]^{2+}$. Evidence that this series is generated by ligand-based redox reactions has been obtained from a detailed analysis of the EPR spectrum of the spin-doublet nickel cation, for which over 80 hyperfine lines are resolved and $\langle g \rangle = 2.001$. With the aid of selectively deuterated derivatives ligand hyperfine coupling constants were obtained which afford accurate simulations of experimental spectra. Spin densities estimated from the coupling constants indicate that the unpaired electron in $[Ni(L)]^+$ is predominantly located on the ligand. This result together with other considerations strongly supports the description of the electron transfer series as $[M^{II}L^{2-}(16\pi)]^0 \rightleftharpoons [M^{II}L^{\cdot -}(15\pi)]^+ \rightleftharpoons [M^{II}L^0(14\pi)]^{2+}$. Oxidation state changes are effectively confined to the ligand system, which is a tetraaza[14]annulene.

A critical matter in interpreting the electron transfer reactions of metal complexes, particularly with regard to the number of detectable species coupled in redox chains whose members are interrelated by one-electron processes,[1-3] is the identification of sites within a molecule which undergo significant changes in oxidation level upon passing from one redox state to another. In a simplified limiting sense many of these reactions can be interpreted in terms of localized oxidation state changes of the metal or, where possible, of the ligand system. This situation is illustrated in eq 1 for the neutral metal(II) complex **1** containing a closed shell dinegative ligand system. Conceivably, electron transfer could

$$\begin{matrix}[M^{I}L^{2-}]^- \\ \mathbf{2} \\ [M^{III}L^{3-}]^- \\ \mathbf{4}\end{matrix} \overset{+e^-}{\leftarrow} [M^{II}L^{2-}] \overset{-e^-}{\rightarrow} \begin{matrix}[M^{III}L^{2-}]^+ \\ \mathbf{3} \\ [M^{II}L^{\cdot -}]^+ \\ \mathbf{5}\end{matrix} \qquad (1)$$

result in changes in the metal oxidation state (**2**, **3**) or in oxidation or reduction of the ligand without an effective change at the metal (**4**, **5**). Further redox reactions of **2**–**5** are also possible. Whereas metal-centered redox reactions are entirely common, processes of the second type are much less frequently encountered. Probably the most convincing demonstration of ligand-based electron-transfer reactions is derived from EPR studies of the one-electron redox products of a species such as **1**. Barring any internal metal–ligand electron rearrangements,[4] the appearance of hyperfine splitting patterns indicative of a high degree of electron delocalization constitutes reasonable evidence that the hole created in oxidation or the electron added in reduction directly alters the original oxidation level of the ligand.

Among general classes of redox-active metal complexes, ligand-based electron transfer reactions have been most comprehensively demonstrated with the metalloporphyrins,[9-14] especially those of Zn(II), Mg(II), and Ni(II). For example, oxidation of type **1** complexes affords stable monocations whose well-developed EPR spectra fully support the cation-radical formulation **5** and have allowed deduction of electronic ground states.[10,12-14] Among other tetraazamacrocyclic complexes the redox properties of those containing Ni(II) have been the most thoroughly investigated. Many of these complexes form three-membered electron transfer series, with the oxidized form containing Ni(III) and the reduced form Ni(I) or a Ni(II)–radical anion arrangement depending on the extent of ligand unsaturation.[15,16] At a position somewhat intermediate between cases of essentially pure metal- and ligand-based electron transfer, but biased toward the latter, are the metal dithiolenes and related complexes,[1-3,17,18] all of which exhibit from two to five total oxidation levels. Detailed EPR studies of $[Ni(mnt)_2]^-$ [19,20] and other dithiolenes[19,21] indicate strong metal–ligand covalency and the consequent desirability of a MO description of charge distribution. However, the existence of five-membered electron transfer series can be rationalized by combinations of the three distinct ligand oxidation states bound to a metal such as Ni(II).[1,2]

Pertinent to the question of redox sites in electron transfer chains is the three-membered series $M(Me_4[14]hexaenatoN_4]$ (**6**) $\rightleftharpoons$ $[M(Me_4[14]hexaenatoN_4)]^+$ (**7**) $\rightleftharpoons$ $[M(Me_4[14]heptaenatoN_4)]^{2+}$ (**8**).[22] The synthesis of **6**

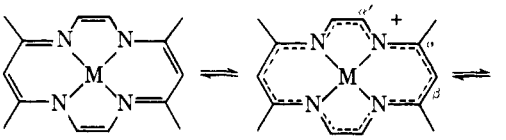

6 **7**

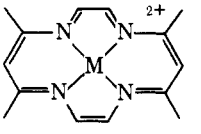

8

and **7** and electrochemical definition of the series with M = Ni and Cu have been previously reported;[24] corresponding work on the palladium complexes has been described by Truex.[25] Based on consideration of electrochemical and other results, it was proposed[24,25] that the above series is generated by ligand-based redox reactions in which the tetraazaannulene-type ligand system exists in three oxidation levels, **6** (16-π), **7** (15-π), and **8** (14-π), each stabilized

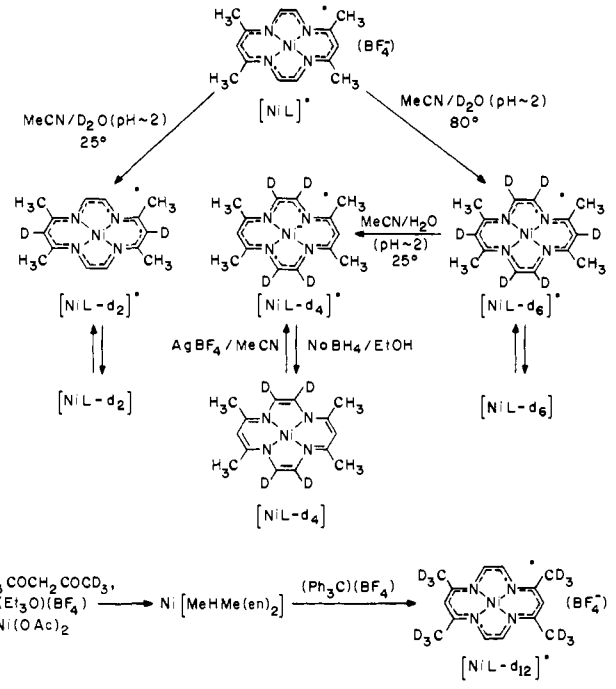

Figure 1. Scheme illustrating the synthesis of d_2, d_4, and d_6 derivatives of $[Ni(Me_4[14]hexaenatoN_4)]^+$ ($[Ni(L)]^+$) by H/D exchange reactions at the β- and α'-C positions, the direct synthesis of the d_{12} derivative, and cation reduction to $[Ni(L\text{-}d_n)]$.

by coordination to M(II). In this description **6** and **7** are equivalent to **1** and **5**, respectively. A necessary consequence of this proposal is a high degree of localization of the unpaired electron on the ligand framework in monocation **7**, a matter not adequately investigated previously.[24] This report presents a detailed analysis of the EPR spectrum of the nickel monocation which has led to a semiquantitative evaluation of electron distribution and probable ground state identification. Certain of the results presented here have been briefly summarized elsewhere.[26]

Experimental Section

Preparation of Compounds. $Ni(Me_4[14]hexaenatoN_4)$,[24] $[Ni(Me_4[14]hexaenato)](BF_4)$,[24] $Pd(Me_4[14]hexaenatoN_4)$,[25] and $[Pd(Me_4[14]hexaenatoN_4)](BF_4)$[25] were prepared as previously described. All manipulations in the following syntheses were performed under a dry dinitrogen atmosphere.

$[Ni(Me_4[14]hexaenatoN_4)](CF_3SO_3)$. To a slurry of 1.0 g (3.2 mmol) of the tetrafluoroborate salt was added 0.80 g (3.2 mmol) of silver trifluoromethanesulfonate dissolved in 30 ml of acetonitrile. An immediate color change from orange to green concurrent with the precipitation of some colloidal silver was observed. The mixture was stirred for 1 hr, filtered, and the residue was washed with hot degassed acetonitrile until the filtrate was colorless. Evaporation of the solvent under reduced pressure and recrystallization of the residue from acetonitrile afforded 0.70 g (50%) of black crystals, mp 276–277° (uncorr). Anal. Calcd for $C_{15}H_{18}F_3N_4O_3SNi$: C, 40.03; H, 4.03; N, 12.45. Found: C, 40.26; H, 4.02; N, 12.47.

Deuterated Derivatives of $[Ni(Me_4[14]hexaenatoN_4)]^+$. Reactions leading to various deuterated derivatives, $[Ni(L\text{-}d_n)]^+$, together with the structural formulas of certain of these species, are set out in Figure 1. H/D and D/H exchange reactions at the β and α' ring positions (**7**) were performed directly on the cations. In several cases the extent of deuterium enrichment was assayed by integration of the ^1H NMR spectra of the diamagnetic complexes $[Ni(L\text{-}d_n)]$ (cf. Figure 2), obtained by borohydride reduction[24] of the corresponding cation. One typical reduction procedure is described.

(a) $[Ni(Me_4[14]hexaenatoN_4)\text{-}d_2](BF_4)$. To a solution of 0.5 g of $[Ni(L)](BF_4)$ in 500 ml of acetonitrile was added 5 ml of D_2O adjusted to pH ~2. The solution was stirred at 25° for 3 hr followed by the addition of 200 ml of anhydrous diethyl ether to precipitate the product, $[Ni(L\text{-}d_2)](BF_4)$, which was isolated by filtration as a green powder with essentially quantitative recovery.

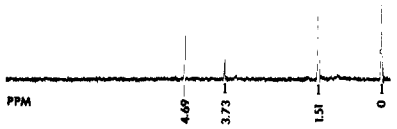

Figure 2. ^1H NMR spectrum (90 MHz) of $Ni(Me_4[14]hexaenatoN_4)$ in CS_2 solution. Chemical shifts are downfield of TMS and are assigned to CH_3, β-H, and α'-H in order of increasing downfield displacement.

(b) $Ni(Me_4[14]hexaenatoN_4)\text{-}d_2$. To $[Ni(L\text{-}d_2)](BF_4)$ (100 mg, 0.20 mmol) suspended in 15 ml of ethanol-d_1 was added ca. 8 mg (0.2 mmol) of $NaBH_4$. The mixture was stirred for 30 min and filtered to give 39 mg (64%) of product, $[Ni(L\text{-}d_2)]$, whose ^1H NMR spectrum indicated >95% deuterium incorporation into $[Ni(L)]^+$ (previous preparation).

(c) $[Ni(Me_4[14]hexaenatoN_4)\text{-}d_6](BF_4)$. A solution of 1.0 g of $[Ni(L)](BF_4)$ and 1 ml of D_2O (pH ~2) in 150 ml of acetonitrile was refluxed for 45 min. (Prolonged heating or the addition of a larger quantity of D_2O causes extensive decomposition of starting material.) After cooling the solution to 0° and filtration the product was recovered as black crystals (0.60 g, 60%), mp 260–262°. Repetition of this procedure followed by reduction of $[Ni(L\text{-}d_6)]^+$ in ethanol-d_1 indicated ≳95% deuteration at β- and α'-C.

(d) $[Ni(Me_4[14]hexaenatoN_4)\text{-}d_4](BF_4)$. This compound was prepared in situ. A solution of 10–15 mg of $[Ni(L\text{-}d_6)](BF_4)$ and ca. 10 drops of water (pH ~2) in 10 ml of acetonitrile was stirred for 30 min at 25°. Dichloromethane (40 ml) was added and the resulting solution was transferred via cannula to an EPR tube. This procedure gave consistent EPR spectral results ascribable to $[Ni(L\text{-}d_4)]^+$ (see text).

(e) $[Ni(Me_4[14]hexaenatoN_4)\text{-}d_{12}](BF_4)$. This compound was prepared by the following reaction sequence in which the extent of methyl group deuteration was monitored by ^1H NMR. Ethyl acetate-d_3 (ca. 89% deuterium enriched), obtained in high yield from the reaction[27] of ethyl iodide and silver acetate-d_3,[28] was condensed with commercial acetone-d_6 (99+% enriched) in the presence of sodium hydride[29] to afford in good yield 2,4-pentanedione-d_6 (ca. 88% enriched). Reaction of the latter with neat ethylenediamine[30] gave bis(acetylacetone)ethylenediimine-d_{12} (ca. 88% enriched), which was O-alkylated and cyclized with ethylenediamine[31] to yield the macrocycle $H_2(Me_4[14]tetraeneN_4)\text{-}d_{12}$ with the same level of enrichment. Reaction with $Ni(OAc)_2{\cdot}4H_2O$ in refluxing methanol[24] afforded $Ni(Me_4[14]tetraenatoN_4)\text{-}d_{12}$ (ca. 90% enriched). The latter (1.5 g, 4.8 mmol) was subjected to oxidative dehydrogenation[24] by stirring with trityl tetrafluoroborate (4.7 g, 14 mmol) in 50 ml of acetonitrile at 80° for 1 hr. After cooling to 0° the dark precipitate was collected, washed with hot ethanol (3 × 100 ml) and dichloromethane (3 × 100 ml), and recrystallized from acetonitrile–methanol to give 0.90 g (47%) of the product, $[Ni(L\text{-}d_{12})](BF_4)$, mp 261–262°, lit.[24] 262–263°. The ^1H NMR spectrum of the reduction product, $[Ni(L\text{-}d_{12})]$, indicated ca. 85% deuterium enrichment of the methyl groups and no deuterium at other positions.

(f) $[Ni(Me_4[14]hexaenatoN_4)\text{-}d_{14}](BF_4)$. β-Deuterium enrichment of $[Ni(L\text{-}d_{12})]^+$ was carried out in situ using a procedure analogous to that for $[Ni(L\text{-}d_2)]^+$.

(g) $[Ni(Me_4[14]hexaenatoN_4)\text{-}d_{18}](BF_4)$. A solution of 200 mg of $[Ni(L\text{-}d_{12})](BF_4)$ in 25 ml of acetonitrile and 10 drops of D_2O (pH ~2) was heated at reflux for 1 hr. The reaction mixture was cooled to 0° and the product, $[Ni(L\text{-}d_{18})](BF_4)$, (110 mg, 55%), was isolated as black crystals, mp 260–263°.

(h) $[Ni(Me_4[14]hexaenatoN_4)\text{-}d_{16}](BF_4)$. β-Hydrogen enrichment of $[Ni(L\text{-}d_{18})]^+$ was carried out in situ using a procedure analogous to that for $[Ni(L\text{-}d_4)]^+$.

Physical Measurements. ^1H NMR spectra were obtained on a Varian T-60 or an Hitachi Perkin-Elmer R-22B spectrometer. EPR spectra were determined using a Varian E-9 spectrometer operating at X-band frequencies. The magnetic field was monitored with a Harvey-Wells Precision NMR gaussmeter (Model G-502)

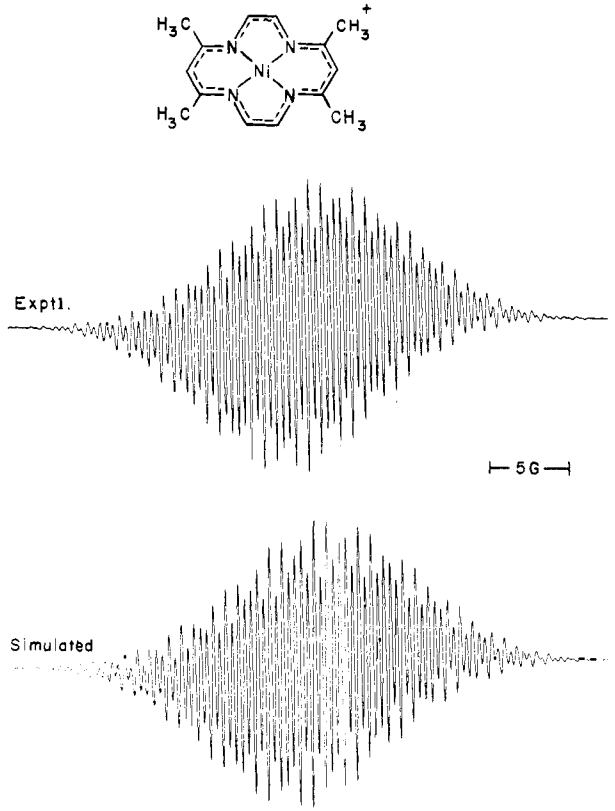

Figure 3. First derivative EPR spectra of $[Ni(L)]^+$ in CH_3CN-CH_2Cl_2: upper, experimental; lower, computer-simulated using the coupling constants in Table I, Lorentzian line shape, and 0.28 G line width.

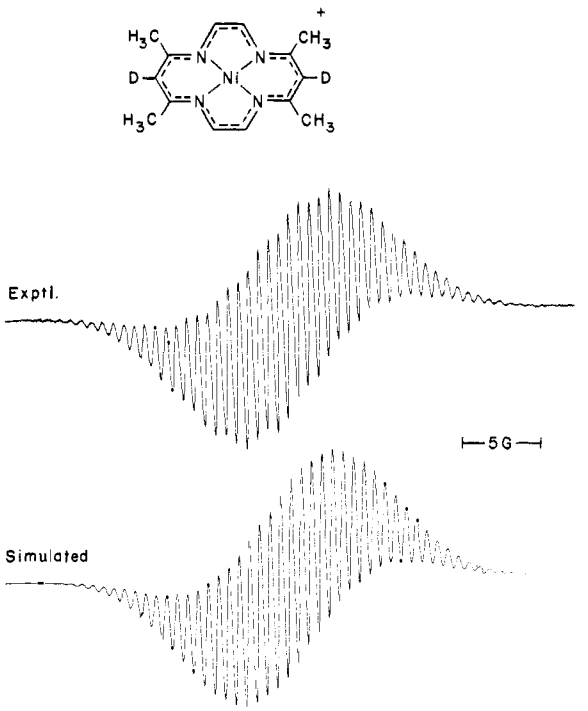

Figure 4. First derivative EPR spectra of $[Ni(L\text{-}d_2)]^+$ in CH_3CN-CH_2Cl_2: upper, experimental; lower, computer-simulated as in Figure 3 but with $a_{\beta D} = 0.70$ and 0.40 G line width.

and the microwave frequency was measured with a Sperry microline frequency meter (Model 1241), the accuracy of which was checked using a perylene-H_2SO_4 solution at different operating frequencies. All solutions for EPR examination were prepared in the absence of oxygen using degassed solvents. The concentration dependence of resonance line shapes was investigated using ca. 10^{-2} to 10^{-4} M acetonitrile solutions at ambient temperature in a Varian E-248 flat aqueous solution cell. All other spectra were obtained at ~25° with ca. 5×10^{-4} M solutions using 4/1 v/v dichloromethane-acetonitrile solvent and contained in quartz tubes. Line shapes at this concentration were not significantly affected by substitution of another nonaqueous solvent for dichloromethane nor by lowering the temperature.

EPR Line Shapes and Computer Simulation. The spectra of $[Ni(L\text{-}d_n)](BF_4)$, n = 0, 2, 4, 6, 12, 14, 16, 18, were recorded in both first and second derivative modes. First derivative spectra of the n = 0, 2, 4, 6, and 12 species are displayed in Figures 3-7. Second derivative spectra of the n = 12, 14, and 16 species are shown in Figure 8. All spectra were recorded under comparable spectrometer settings and their features are briefly described.

$[Ni(L)]^+$: ≥80 resolved lines with a nearly constant spacing of 0.41 G (Figure 3); $\langle g \rangle = 2.001$.

$[Ni(L\text{-}d_2)]^+$: ≥45 resolved lines with a spacing of ca. 0.7 G and increased line broadening compared to the d_0 case (Figure 4).

$[Ni(L\text{-}d_4)]^+$: ≥70 resolved lines with a nearly constant spacing of 0.41 G; except for intensity differences this spectrum is almost superimposible with that of $[Ni(L)]^+$ (Figure 5).

$[Ni(L\text{-}d_6)]^+$: Single Gaussian curve, peak-to-peak line width of 9.2 G, and poorly resolved hyperfine splitting (Figure 6).

$[Ni(L\text{-}d_{12})]^+$: 15 resolved lines separated by ca. 2.3 G (Figures 7 and 8).

$[Ni(L\text{-}d_{14})]^+$: ~11 resolved lines separated by ca. 2.2 G; resolution is better in the second derivative spectrum (Figure 8).

$[Ni(L\text{-}d_{16})]^+$: Nine resolved lines separated by 2.1-2.2 G; resolution is better in the second derivative spectrum (Figure 8).

$[Ni(L\text{-}d_{18})]^+$: single Gaussian curve, peak-to-peak line width of 9.0 G, and no resolved hyperfine splitting.

The computer program employed for simulation of EPR spectra was obtained from Dr. H. van Willigen and is similar to that described by Stone and Maki.[32] Input parameters consist of hyperfine coupling constants, nuclear spins, line widths, line shape functions (Gaussian or Lorentzian), and phase and dimensional parameters for the plotting routine.

Results and Discussion

It has been previously reported that the EPR spectrum of $[Ni(L)]^+$ in DMF-acetone solution consisted of a single line with poorly resolved hyperfine splitting.[24] The solution g value, $\langle g \rangle = 2.002$, and the lack of observable g anisotropy in a frozen solution are inconsistent with the presence of Ni(III)[16,19,20] as in **3** and were interpreted[24] in terms of the limiting cation radical formulation **5**. However, the failure to resolve hyperfine structure was disturbing. Limited information available at that time,[24] augmented since by more extensive studies,[25,33] reveals that the solution chemistry of $[Ni(L)]^+$ and its palladium analog is complicated by the presence of an apparent paramagnetic monomer ⇌ diamagnetic dimer equilibrium. Consequently, the ill-resolved spectral feature could have resulted from electron transfer between monomer and dimer, or possibly from spin-exchange narrowing in the event of an inappropriately high monomer concentration. In order to ascertain the EPR spectrum of the monomer uncomplicated by such effects, a study of the concentration dependence of the line shape of $[Ni(L)](BF_4)$ was performed. Over the interval of ca. 10^{-2} to 10^{-4} M, hyperfine structure became increasingly well resolved with decreasing concentration until at ca. 5×10^{-4} M the limiting spectrum was obtained.

The well-resolved limiting spectrum of $[Ni(L)](BF_4)$ in 4/1 v/v CH_2Cl_2-CH_3CN solution is shown in Figure 3. Over 80 lines are evident; assuming D_{2h} cation symmetry the theoretical number of lines is 1755[34] if the four coupling constants $a_{\beta H}$, $a_{\alpha' H}$, a_{Me}, and a_N are unequal. To ensure that the splitting pattern did not arise in part from coupling to the fluorine nuclei of the anion, the spectrum of the $CF_3SO_3^-$ salt was investigated and found to be identical with that of the BF_4^- salt at the same concentration. Such coupling conceivably could occur in the event of ion pair

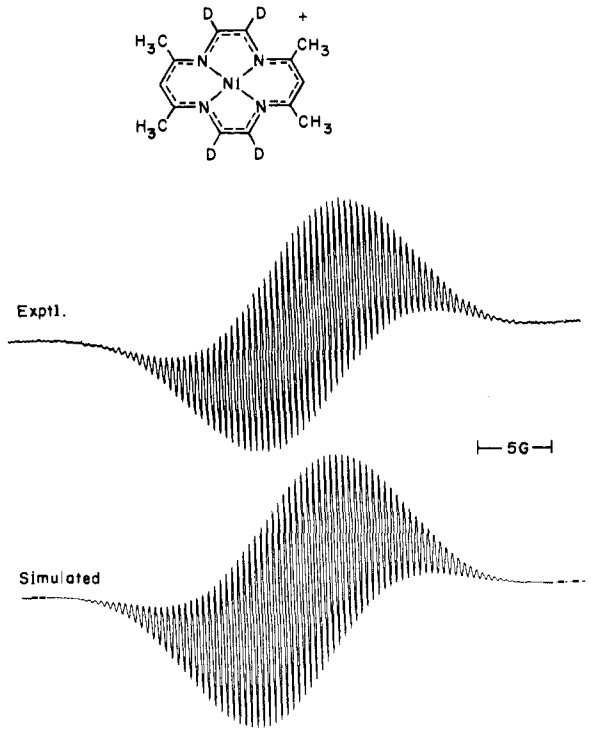

Figure 5. First derivative EPR spectra of $[Ni(L\text{-}d_4)]^+$ in CH_3CN-CH_2Cl_2: upper, experimental; lower, computer-simulated as in Figure 3 but with $a_{\alpha'D} = 0.44$ and 0.35 G line width.

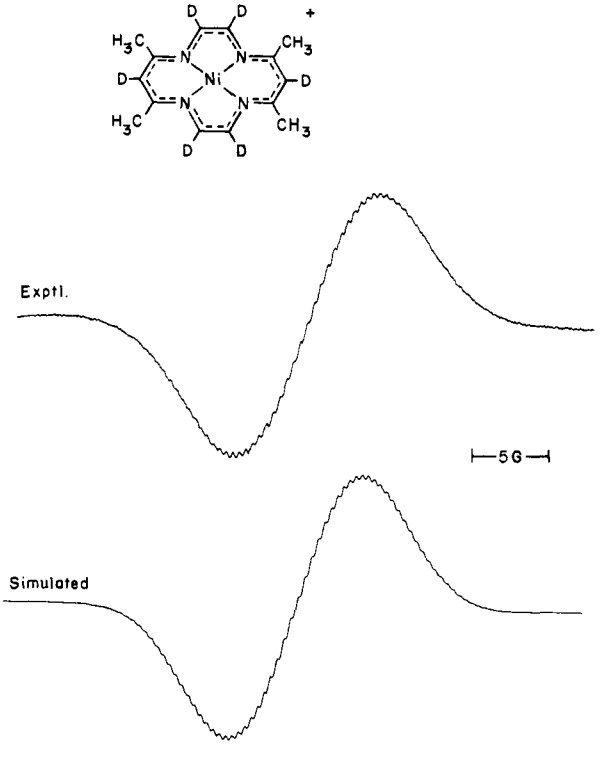

Figure 6. First derivative EPR spectra of $[Ni(L\text{-}d_6)]^+$ in CH_3CN-CH_2Cl_2: upper, experimental; lower, computer-simulated as in Figure 5 but with $a_{\beta D} = 0.70$ G.

formation and has been observed with halide salts of $[Zn(TPP)]^+$.[10] The observed splittings are concluded to derive entirely from ligand nuclei. The nearly constant spacing of 0.41 G between all components in Figure 3 suggested that the coupling constants are near-integral multiples of this spacing. However, the complexity of the spectrum did not allow extraction of any one coupling constant with certainty.

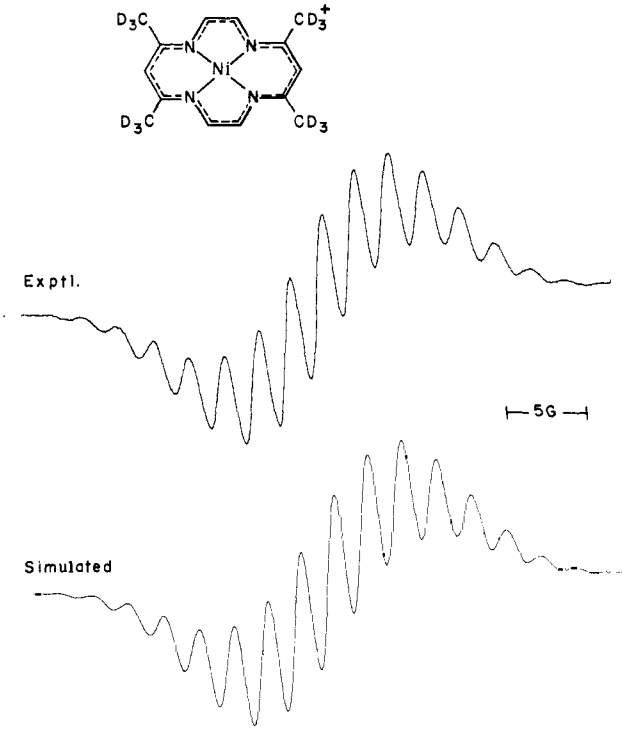

Figure 7. First derivative EPR spectra of $[Ni(L\text{-}d_{12})]^+$ in CH_3CN-CH_2Cl_2; upper, experimental; lower, computer-simulated as in Figure 3 but with $a_{CD_3} = 0.124$ and 0.80 G line width.

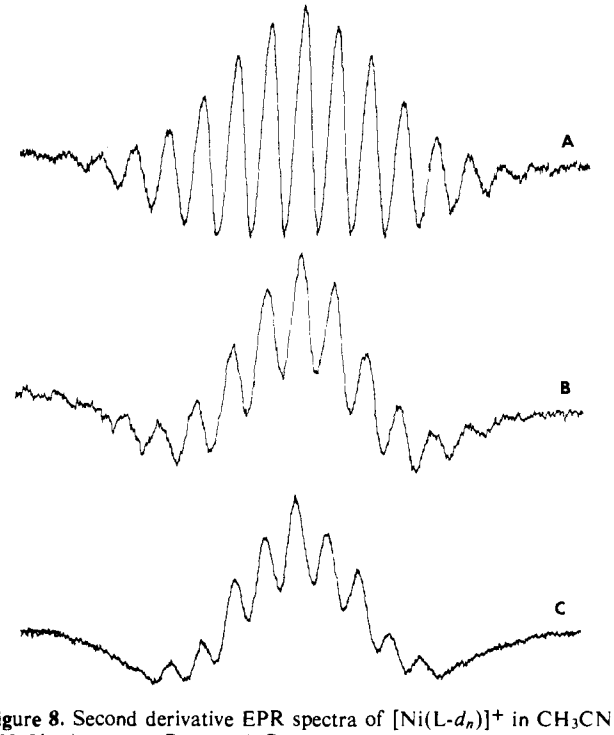

Figure 8. Second derivative EPR spectra of $[Ni(L\text{-}d_n)]^+$ in CH_3CN-CH_2Cl_2: A, $n = 12$; B, $n = 14$; C, $n = 16$.

Deuterated Derivatives of $[Ni(L)]^+$. As a means of altering the spectrum of $[Ni(L)]^+$ such that one or more coupling constants could be possibly determined or estimated, a series of deuterated derivatives $[Ni(L\text{-}d_n)]^+$, $n = 2, 4, 6, 12, 14, 16, 18$, having deuterium enrichment at specific ligand positions was prepared (Figure 1). The robust nature of the cation allowed preparation of the $n = 2$ [2(βD)], $n = 6$ [2(βD) + 4 (α′D)], and $n = 4$ [4(α′D)] species by direct D/H or H/D exchange under the indicated conditions without evident decomposition. The ring system of the cation is

Table I. Coupling Constants and Experimentally Estimated Spin Densities for $[Ni(L)]^+$; HMO and McLachlan Spin Densities for the $3b_{1u}$ Orbital of the Tetramethyltetraaza[14]annulene Ligand System

Position	$\lvert a\rvert$, G[a]	ρ[b]	I[c]		II[c]		III[c]	
			HMO	McL	HMO	McL	HMO	McL
N	2.08	(+)0.087	+0.116	+0.165	+0.100	+0.141	+0.083	+0.110
$C-CH_3$	0.81	(−)0.021	+0.001	−0.057	0	−0.059	+0.002	−0.049
β-C	4.53	(+)0.168	+0.109	+0.130	+0.100	+0.098	+0.074	+0.023
α'-C	2.87	(+)0.106	+0.078	+0.077	+0.100	+0.141	+0.129	+0.177
$E(\beta)$			−0.217		0		0.361	

[a] Set of best-fit values from spectra simulated. [b] Calculated from Q values given in text. [c] Parameter sets for $\alpha_N = \alpha + h\beta$, $\beta_{CN} = k\beta$; I (pyridine type-N), $h = 0.5$, $k = 1.0$; II (porphyrin type-N), $h = k = 1.0$; III (pyrrole type-N), $h = 1.5$, $k = 0.8$. In each set $\alpha_{CCH_3} = \alpha - 0.5\beta$, $\beta_{CCH_3} = 0$.

subject to electrophilic attack, and the particularly facile deuteration at β-C is foreshadowed by reports that the 6-π β-iminoaminato chelate ring in various Ni(II) complexes can be protonated[35,36] and is reactive toward other electrophiles[36] at this position. Unlike the $CH_3C{=}N$-groups in cationic Ni(II) complexes of Curtis 4-π macrocycles,[37] the α-methyl groups of $[Ni(L)]^+$ do not undergo ready base-catalyzed H/D exchange. Under such conditions substantial decomposition of the cation was observed. The same result was obtained in attempts to deuterate the precursor ligand $H_2(Me_4[14]tetraeneN_4)$.[22,24] The perdeuteriomethyl complex $[Ni(L\text{-}d_{12})]^+$ was prepared by the reaction sequence described previously[24,31] starting from 2,4-pentadione-d_6. The conditions outlined in Figure 1 were used for specific deuterium labeling of $[Ni(L\text{-}d_{12})]^+$, yielding the $n = 14$ [2(βD)], $n = 16$ [4(α'D)], and $n = 18$ [2 (βD) + 4 (α'D)] species. Where assayed from the ^1H NMR spectra of $[Ni(L\text{-}d_n)]$, obtained by borohydride reduction, deuterium enrichment in the cations is ≥95% at the β and α' ring positions and ca. 85% in the methyl groups.

Spectral Analysis. The introduction of deuterium ($I = 1$, $a_D = 0.1535a_H$) at positions of nonnegligible spin density should afford detectable changes in line shapes whose exact forms will depend on the relative magnitudes of coupling constants and spectral resolution. When the EPR spectra of $[Ni(L\text{-}d_n)]^+$ ($n = 2$, 4, 6, 12, 14, and 16, Figures 4–8) are compared with the spectrum of the undeuterated cation (Figure 3), appreciable changes are revealed in each case. These results indicate that each of the three sets of ligand protons is observably coupled to the odd electron, a probable situation only if the electron is π-delocalized. Spectra of the $n = 12$, 14, and 16 species (Figures 7 and 8), all of which are perdeuteriomethylated, display from 9 to 15 resolved but broadened lines separated by 2.1–2.3 G. From these spectra it appeared that $a_{CD_3} \lesssim 1/20$ of the line width (ca. 1.5 G), leading to the estimate that $a_{CD_3} \lesssim 0.1$ G, or $a_{CH_3} \lesssim 0.7$ G. The second derivative spectrum of $[Ni(L\text{-}d_{16})]^+$ consists of nine resolved lines separated by 2.1–2.2 G with an intensity pattern approximately but not exactly that expected from coupling with four equivalent ^{14}N nuclei ($I = 1$). This spectrum suggested that $a_N \sim 2.1$–2.2 G. Comparative spectra of this species and $[Ni(L\text{-}d_{14})]^+$ further suggested that $a_{\beta H}$ is larger than and possibly an approximate multiple of a_N, and led to the trial values $a_{\beta H} \sim 4.4$–4.6 G.

The highly resolved spectra of $[Ni(L\text{-}d_2)]^+$ (Figure 4) and $[Ni(L\text{-}d_4)]^+$ (Figure 5) were examined in terms of several initial assumptions concerning ring proton coupling constants. However, noting that the nearly constant separation of 0.7 G for $[Ni(L\text{-}d_2)]^+$ is consistent with the above estimate of $a_{\beta H}$, this splitting was assigned to $a_{\beta D}$ affording $a_{\beta H} \simeq 4.6$ G. The spectrum of $[Ni(L\text{-}d_4)]^+$ contains a spacing of 0.41 G between all hyperfine components. This value is selected as $a_{\alpha'D}$, leading to $a_{\alpha'H} \simeq 2.7$ G. If a_{CH_3} is taken as 0.7 G the values of a_{CH_3}, a_N, $a_{\alpha'H}$, and $a_{\beta H}$ are not all integral multiples (1.8:5.2:6.6:11) of the nearly constant 0.41 G separation observed in the $[Ni(L)]^+$ spectrum.

The preceding coupling constants were tested by their employment in computer simulations of the spectra of $[Ni(L)]^+$ and its deuterated derivatives. The later sets of values tested were constrained to be near-integral multiples of 0.41 G. The final set of coupling constants is listed in Table I and afforded extremely close spectral simulations, which are shown in Figures 3–7. While it cannot be claimed that this parameter set is unique in the synthesis of a spectrum as complex as that of $[Ni(L)]^+$, we have been unable to find by extensive computer analysis any other set which is adequate.[38] In particular, taking $a_{CH_3} = 0.41$ G or using integral multiples of 0.41 G other than the 5:2:1:7 relationship evident in Table I was not successful.

Electronic Structure of $[Ni(L)]^+$. Under the D_{2h} symmetry of $[Ni(L)]^+$ established by the preceding spectral analysis, the 14 p-π ligand orbitals transform as $\Gamma_\pi = 3B_{2g} + 3A_u + 4B_{1u} + 4B_{3g}$ and the metal orbitals as A_g ($d_{x^2-y^2}$, d_{z^2}), B_{1g} (d_{xy}), B_{2g} (d_{xz}), B_{3g} (d_{yz}), B_{1u} (p_z), B_{2u} (p_y), and B_{3u} (p_x).[39] As a guide to the probable energy ordering of π-MO's of the tetramethyltetraaza[14]annulene ligand system, a series of HMO calculations was performed with a range of parameters selected on the basis of suggestions by Streitweser[40] and work on prophyrins.[41] Parameter sets I, II, and III are defined in Table I. Regardless of the parameterization of nitrogen coulomb and resonance integrals employed within the range of these sets, the MO ordering proved to be invariant. This order may be altered by the presence of the coordinated metal, but any deviations from pure ligand orbital energy ordering is difficult to predict without a meaningful calculation for the entire complex. Consequently, the assumption is made in arriving at a ground state description of $[Ni(L)]^+$ that the only significant effects of the metal are those involving the highest filled and half-filled and lowest vacant MO's. HMO results predict the order $\ldots (2b_{2g})^2(3b_{1u})^1(2a_u)^0 \ldots$, with the $3b_{1u}$ orbital ranging from weakly bonding to weakly antibonding (Table I).

Ligand π spin densities were estimated from HMO and McLachlan[42] calculations. The latter introduces electron correlation and is useful in predicting sites of negative spin densities. HMO calculations indicate the following orders of spin densities in the $2b_{2g}$ and $2a_u$ orbitals: $\rho_{\alpha'C} > \rho_{CCH_3} \gtrsim \rho_N > \rho_{\beta C} = 0$ ($2b_{2g}$), and $\rho_{CCH_3} > \rho_{\alpha'C} > \rho_N(\sim 0) > \rho_{\beta C} = 0$ ($2a_u$). Both orbitals contain a node at β-C which will persist in $2b_{2g}$ even with metal (d_{xz})-ligand mixing; $2a_u$ is nonbonding with respect to all metal orbitals. The experimental result that $a_{\beta H} \gg a_{CH_3}$, together with $|\rho_{\beta H}| \gg |\rho_{CCH_3}|$ estimated from Q values given below makes it improbable that the half-filled orbital is $2b_{2g}$ or $2a_u$.

The experimental coupling constants have been used to estimate spin densities in $[Ni(L)]^+$ from the usual equation $a = Q\rho$, with $Q_{CH} = -27$, $Q_{CCH_3} = 39$, and $Q_N = 24$ G. Spin densities obtained from these values, which have been

previously employed for metalloporphyrin[10,14,43] and other cation radicals, are collected in Table I together with results obtained by the HMO and McLachlan procedures for the $3b_{1u}$ ligand orbital. All three parameter sets predict substantial spin density at N and α'-C and small spin density at C-CH_3. Relative spin densities at β-C and α'-C are rather parameter-dependent with a small $\rho_{\beta C}$ value obtained with set III. Close agreement between experimentally estimated and calculated spin densities is not found, nor can such be expected in view of the approximations inherent in the calculations, omission of perturbative effects of the metal,[44] and uncertainties in the best values of Q.[45] However, only for the $3b_{1u}$ orbital are substantial spin densities predicted simultaneously for N, α'-C, and β'-C (excluding set III) over a reasonable range of parameters. From these considerations it is concluded that $^2B_{1u}$ is the most probable ground state of $[Ni(L)]^+$. If the preceding Q values are accepted as reasonable, the sum of the estimated signed spin densities from experiment is 1.02, close to the required value of unity if the unpaired electron is exclusively ligand based. Because of the uncertainties in Q values, this sum, as the indidividual spin densities, cannot be accorded any strictly quantitative significance. However, it is considered indicative of the dominant ligand nature of the electron. Some finite spin density at nickel could arise directly by mixing of the $3b_{1u}$ ligand orbital with the vacant $4p_z$ metal orbital, the only symmetry permitted ligand-metal interaction. Evidently the metal component of the bonding MO of the complex derived from this interaction is not appreciable.

Evidence for a Ligand-Based Electron Transfer Series. The preceding analysis of the EPR spectrum of $[Ni(L)]^+$ indicates that the ground state of this complex is $^2B_{1u}$ with an electron distribution which closely approaches the formalism $[Ni^{II}L^{\cdot -}\ (15\pi)]^+$ (**5**). The establishment of $[Ni(L)]^+$ as, effectively, a metal(II) complex of a 15-π tetraazannulene ligand gives credence to the proposal that individual members of the three-membered electron transfer chain **6–8** are related by ligand-based redox reactions as shown in series 2.

$$[Ni^{II}L^{2-}\ (16\pi)]^0 \rightleftharpoons [Ni^{II}L^{\cdot -}\ (15\pi)]^+ \rightleftharpoons [Ni^{II}L^{0}\ (14\pi)]^{2+} \quad (2)$$
$$\mathbf{6} \qquad\qquad \mathbf{7} \qquad\qquad \mathbf{8}$$

By analogy the same description may also apply to the electron transfer series $[M(L)]^{0,+,2+}$ with M = Cu(II)[24] and Pd(II).[25] Further evidence bearing on the ligand-based nature in these two and the nickel series is briefly summarized.

(i) **EPR Results.** The EPR spectrum of $[Pd(L)]^+$ was obtained in 4/1 v/v CH_2Cl_2-CH_3CN and showed an extensive hyperfine pattern of over 70 lines which differs in fine detail of line spacings and relative intensities from the $[Ni(L)]^+$ spectrum in Figure 3. Deuterated derivatives were not prepared, and the spectrum was not analyzed. The spectrum is indicative of substantial ligand character as is $\langle g \rangle$ = 1.998; reduction below the free electron value (2.002) is slight.

(ii) **Redox Potentials.** Polarographic half-wave potentials have been correlated with π-MO energies in a wide variety of conjugated and aromatic compounds including nitrogen heterocycles.[46] In instances where metal complexes undergo two successive one-electron reactions, a frequently employed criterion for small or zero metal character in the orbitals involved is an approximately constant difference in potentials when the metal is varied. Thus for the metalloporphyrin series (3), in which ligand redox has been estab-

$$[M^{II}P^{2-}\ (26\pi)] \rightleftharpoons [M^{II}P^{\cdot -}\ (25\pi)]^+ \rightleftharpoons [M^{II}P^{0}\ (24\pi)]^{2+} \quad (3)$$

lished by EPR and electronic spectral results, $\Delta E_{1/2} = E_{1/2}(2+/+) - E_{1/2}(+/0) = 0.3 \pm 0.1$ V for different M(II).[13] Likewise, in four series of bis(dithiolenes) $[M(S_2C_2R_2)_2]^z$ with M = Ni, Pd, and Pt $\Delta E_{1/2} = E_{1/2}(0/-) - E_{1/2}(-/2-) = 0.93 \pm 0.09$ V at parity of R.[3,17] For the nitrogen analogs $[M(C_6H_4(NH)_2)_2]^z$ with the same metals $\Delta E_{1/2} = 0.65 \pm 0.09$ V.[1] Other examples can be found in the extensive tabulations of potentials by McCleverty.[3,17] In the $[M(L)]^{0,+,2+}$ series potentials[24,25] for M = Ni(II), Cu(II), and Pd(II) yield $\Delta E_{1/2} = 0.63 \pm 0.09$ V, a result entirely consistent with ligand-based electron transfer. This behavior is also consistent with the apparent failure of [Ni(L)] to fit the empirical Ni(II)/Ni(III) potential correlations developed by Lovecchio et al.[16,47] for other tetraaza macrocyclic complexes.

(iii) Scope of Electron Transfer Series. The concept of a complete electron transfer series of metal complexes containing unsaturated ligands has been introduced previously.[1,2] For dithiolenes and their analogs the series (4) is ter-

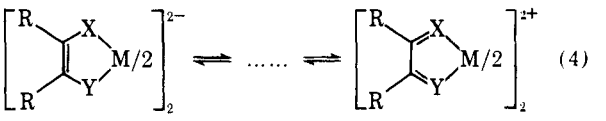

(4)

9 **10**

minated by reduced (**9**) and oxidized (**10**) members with intermediate members having the charges z = 1−, 0, 1+. The scope of the series is five members, all of which can be visualized in terms of distinct ligand oxidation states (dianion, "semi-quinoidal", "quinoidal") in combination with a stable valence state of the metal, here M(II). Several complete series have been demonstrated with M = Ni, Pd, Pt[1,2,48] and X = Y = NH or X = S, Y = NR′. Application of this concept[49] to the $[M(L)]^z$ series predicts three members, as observed, with the electronic structural formalisms given above. In terms of ligand oxidation levels this series finds analogy with the redox properties of *trans*-15,16-dimethyldihydropyrene (DMDHP, **11**). DMDHP (14π) can be re-

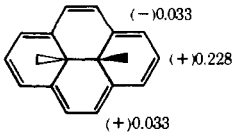

11

duced to $DMDHP^{\cdot -}$ (15π) and $DMDHP^{2-}$ (16π) with $E_{1/2}(0/-) = -1.59$ and $E_{1/2}(-/2-) = -2.15$ V;[51] $\Delta E_{1/2} = 0.56$ V, fortuitously similar to the value for the $[M(L)]^z$ series, with the potential for the first reduction about 2 V more cathodic than the values for $[M(L)]^{2+}$. Experimental spin densities[52] are indicated; signs (from McLachlan calculations) are the same as, and the relatively high $\rho_{\beta C}$ value similar to, $[Ni(L)]^+$. The electronic structure of $DMDHP^{\cdot -}$ is considered in detail elsewhere.[52]

A further possibility exists for examining ligand electron distribution in the $[M(L)]^z$ series. The indicated ligand structures are of the $4n\pi$ ("antiaromatic") and $(4n + 2)\ \pi$ (aromatic) types for [M(L)] and $[M(L)]^{2+}$, respectively. Consequently, the ring protons in the former should become more shielded and those in the latter less shielded[53] relative to a suitable reference, viz., M(Me_4[14]tetraenatoN_4) (**12**),

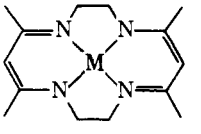

12

which contains two separated 6π chelate rings. Pronounced chemical shift effects of this sort have been found for $DMDHP^{2-/0}$[54] and various nonbridged annulenes.[53] Com-

pared to the shifts of **12** (M = Ni(II),[24] Pd(II)), both the methyl and β-H resonances of [Ni(L)] (Figure 2) and [Pd(L)] are shifted upfield by 0.4 and 0.8 ppm, respectively. Shift differences are not large and, in the absence of data for $[M(L)]^{2+}$, it is difficult to decide if they arise from an induced antiaromatic ring current.[55] Attempts to produce clean chemical generation of the dications by oxidation reactions have thus far proven unsuccessful.

Lastly, the $[M^{II}L^{\cdot-}]^+$ formalism for the monocations **7**, established by the results presented here, is clearly related to that for the metalloporphyrin monocations in series **3**. The latter have two closely spaced highest occupied ligand MO's whose symmetries[9,10,12-14] allow either no mixing with metal orbitals (a_{1u}) or interaction with p_z only (a_{2u}). In view of the symmetry correlation a_{2u} (D_{4h}) $\leftrightarrow$ b_{1u} (D_{2h}), $^2B_{1u}[M(L)]^+$ complexes may be considered the simplest known electronic analogs of $[M(P)]^+$ with the $^2A_{2u}$ ground state.

Acknowledgment. This research was supported by the National Science Foundation under Grant GP-40089X. We thank Dr. J. Fajer for attempts to determine the ENDOR spectrum of $[Ni(L)]^+$, Dr. G. N. LaMar for the McLachlan calculations, and Dr. H. van Willigen for the spectral simulation program and helpful discussions.

References and Notes

(1) A. L. Balch and R. H. Holm, *J. Am. Chem. Soc.*, **88**, 5201 (1966).
(2) C. E. Forbes, A. Gold, and R. H. Holm, *Inorg. Chem.*, **10**, 2479 (1971).
(3) J. A. McCleverty in "Reactions of Molecules at Electrodes", N. S. Hush, Ed., Wiley-Interscience, New York, N.Y., 1971, pp 403–492.
(4) A number of cases are now recognized in which internal electron rearrangement occurs during or after electron transfer.[5-8] The properties of the final products, while interpretable by formalisms like those in eq 1, do not necessarily correspond to oxidation state changes in the original complex which are restricted only to the metal *or* to the ligand.
(5) A. Wolberg and J. Manassen, *Inorg. Chem.*, **9**, 2365 (1970).
(6) N. S. Hush and I. S. Woolsey, *J. Am. Chem. Soc.*, **94**, 4107 (1972).
(7) J. A. Ferguson, T. J. Meyer, and D. G. Whitten, *Inorg. Chem.*, 11, 2767 (1972).
(8) N. Takvoryan, K. Farmery, V. Katovic, F. V. Lovecchio, E. S. Gore, L. B. Anderson, and D. H. Busch, *J. Am. Chem. Soc.*, **96**, 731 (1974).
(9) D. Dolphin, Z. Muljiani, K. Rousseau, D. C. Borg, J. Fajer, and R. H. Felton, *Ann. N.Y. Acad. Sci.*, **206**, 177 (1973).
(10) J. Fajer, D. C. Borg, A. Forman, R. H. Felton, L. Vegh, and D. Dolphin, *Ann. N.Y. Acad. Sci.*, **206**, 349 (1973).
(11) G. M. Brown, F. R. Hopf, J. A. Ferguson, T. J. Meyer, and D. G. Whitten, *J. Am. Chem. Soc.*, **95**, 5939 (1973).
(12) D. Dolphin and R. H. Felton, *Acc. Chem. Res.*, **7**, 26 (1974).
(13) J.-H. Fuhrop, *Struct. Bonding (Berlin)*, **18**, 1 (1974).
(14) J. Fajer, D. C. Borg, A. Forman, A. D. Adler, and V. Varadi, *J. Am. Chem. Soc.*, **96**, 1238 (1974).
(15) D. C. Olson and J. Vasilevskis, *Inorg. Chem.*, **8**, 1611 (1969).
(16) F. V. Lovecchio, E. S. Gore, and D. H. Busch, *J. Am. Chem. Soc.*, **96**, 3109 (1974).
(17) J. A. McCleverty, *Prog. Inorg. Chem.*, **10**, 49 (1968).
(18) E. Hoyer and W. Dietzsch, *Z. Chem.*, 11, 41 (1971).
(19) A. H. Maki, N. Edelstein, A. Davison, and R. H. Holm, *J. Am. Chem. Soc.*, **86**, 4580 (1964).
(20) R. D. Schmitt and A. H. Maki, *J. Am. Chem. Soc.*, **90**, 2288 (1968).
(21) R. L. Schlupp and A. H. Maki, *Inorg. Chem.*, **13**, 44 (1974).
(22) As detailed in a recent publication,[23] the nomenclature originally used for these complexes[24] has been discarded in favor of a scheme similar to that employed by Busch and coworkers.[16] Because this paper deals principally with complexes having the same ligand composition, the simplified designation [Ni(L)], $[Ni(L)]^+$, and $[Ni(L)]^{2+}$ for **6**, **7**, and **8**, respectively, are often used in subsequent discussion. Ring positions are denoted in **7**. The (Me_4[14]tetraenatoN$_4$) ligand system mentioned in the Experimental Section was previously called (MeHMe(en)$_2$).[24]
(23) S. C. Tang and R. H. Holm, *J. Am. Chem. Soc.*, **97**, 3359 (1975).
(24) T. J. Truex and R. H. Holm, *J. Am. Chem. Soc.*, **94**, 4529 (1972).
(25) T. J. Truex, Ph.D. Thesis, M.I.T., 1972.
(26) M. Millar and R. H. Holm, *J. Chem. Soc., Chem. Commun.*, 169 (1975).
(27) B. Nolin, *Can. J. Chem.*, **31**, 1257 (1953).
(28) B. Nolin and L. C. Leitch, *Can. J. Chem.*, **31**, 153 (1953).
(29) F. W. Swamer and C. R. Hauser, *J. Am. Chem. Soc.*, **72**, 1352 (1950).
(30) P. J. McCarthy, R. J. Hovey, K. Ueno, and A. E. Martell, *J. Am. Chem. Soc.*, **77**, 5820 (1955).
(31) S. C. Tang, S. Koch, G. N. Weinstein, R. W. Lane, and R. H. Holm, *Inorg. Chem.*, **12**, 2589 (1973).
(32) E. W. Stone and A. H. Maki, *J. Chem. Phys.*, **38**, 1999 (1963).
(33) M. Millar and R. H. Holm, unpublished observations.
(34) Excluding splittings from the isotopes ^{61}Ni ($I = 3/2$), ^{13}C ($I = 1/2$), and ^{15}N ($I = 1/2$), whose natural abundances are 1.3% or less.
(35) J. G. Martin, R. M. C. Wei, and S. C. Cummings, *Inorg. Chem.*, 11, 475 (1972); J. G. Martin and S. C. Cummings, *ibid.*, **12**, 1479 (1973).
(36) C. J. Hipp and D. H. Busch, *J. Chem. Soc., Chem. Commun.*, 737 (1972); *Inorg. Chem.*, **12**, 894 (1973).
(37) L. G. Warner, N. J. Rose, and D. H. Busch, *J. Am. Chem. Soc.*, **90**, 6938 (1968).
(38) This statement applies to the four different types of coupling constants for D_{2h} symmetry of the cation. No attempts have been made to simulate spectra under lower symmetries, including C_{2h} suggested by one referee, because of the larger number of parameters required. The excellent agreement between experimental and calculated spectra indicates D_{2h} symmetry but, strictly speaking, we have not eliminated the possibility of some lower symmetry.
(39) These symmetries refer to a coordinate system with the *y* axis passing through β-C, the *x* axis bisecting the α'C–α'C bond, and the *z* axis normal to the molecular plane.
(40) A. Streitwieser, "Molecular Orbital Theory", Wiley, New York, N.Y., 1961, Chap. 5.
(41) H. Kobayashi, *J. Chem. Phys.*, **30**, 1373 (1959).
(42) A. D. McLachlan, *Mol. Phys.*, **3**, 233 (1960).
(43) J. Fajer, D. C. Borg, A. Forman, D. Dolphin, and R. H. Felton, *J. Am. Chem. Soc.*, **92**, 2982 (1970).
(44) This point could be investigated by analysis of the spectrum of the free ligand $L^{\cdot-}$; attempts to prepare the ligand by metal removal have failed.
(45) For a brief discussion of this point cf. J. E. Wertz and J. R. Bolton, "Electron Spin Resonance: Elementary Theory and Practical Applications", McGraw-Hill, New York, N.Y., 1972, Chapter 5, and references therein.
(46) B. J. Tabner and J. R. Yandle in "Reactions of Molecules at Electrodes", N. S. Hush, Ed., Wiley-Interscience, New York, N.Y., 1971, pp 283–303.
(47) These authors correctly point out that the [oxidation] reactions of $[Ni(TPP)]^0$ should be similar to $[Ni(L)]^0$, but in a subsequent statement they have interchanged the oxidation and reduction behavior of the latter in describing its redox properties.
(48) E. B. Fleischer, A. E. Gebala, and P. A. Tasker, *Inorg. Chim. Acta*, **6**, 72, (1972).
(49) This concept applies to redox series in which electrons added or removed have substantial ligand character and occupy MO's of the entire complex such that the total electron density in the ligand(s) corresponds to one of its distinct oxidation states or an average thereof. The term "complete" is used in this sense and for any series so described further ligand or metal based reactions, involving highly bonding or antibonding orbitals, are not precluded. Such processes would involve potentials much more positive or negative than those required to form the predicted terminal series members. Examples include $[Ni^{II}(mnt)_2]^{3-}$ [50] from $[Ni^{II}(mnt)_2]^{2-}$ ($E_{1/2}$ (2−/3−) −1.7 V vs. $E_{1/2}$ (−/2−) ~+0.2 V, and $[Pd(L)]^-$ [25] from $[Pd(L)]^0$ ($E_{1/2}$ (0/−) −1.8 V vs. $E_{1/2}$ (+/0) +0.1 V).
(50) T. E. Mines and W. E. Geiger, Jr., *Inorg. Chem.*, **12**, 1189 (1973).
(51) A. J. Fry, L. L. Chung, and V. Boekelheide, *Tetrahedron Lett.*, 445 (1974).
(52) F. Gerson, E. Heilbronner, and V. Boekelheide, *Helv. Chim. Acta*, **47**, 1123 (1964).
(53) R. C. Haddon, V. R. Haddon, and L. M. Jackman, *Fortschr. Chem. Forsch.*, **16**, 103 (1971).
(54) R. H. Mitchell, C. E. Klopfenstein, and V. Boekelheide, *J. Am. Chem. Soc.*, **91**, 4931 (1969).
(55) Ligand bond localization is predicted for an antiaromatic 16π ligand system.[53] While the structure of [M(L)] is unknown, that of a Ni(II) octaaza[14]annulene complex,[56] isoelectronic with [Ni(L)] and having the chelate ring size pattern of **8**, exhibits this property.
(56) V. L. Goedken and S.-M. Peng, *J. Am. Chem. Soc.*, **95**, 5773 (1973).